

Study on hot corrosion reactions between SmYbZr₂O₇ ceramic and vanadium pentoxide at temperatures of 600–1000 °C in air

Sa Li, Zhan-Guo Liu, Jia-Hu Ouyang*

National Key Laboratory for Precision Hot Processing of Metals, School of Materials Science and Engineering, Harbin Institute of Technology, 92 West Da-Zhi Street, Nangang District, Harbin 150001, Heilongjiang, China

ARTICLE INFO

Article history:

Received 15 November 2010
Received in revised form 16 July 2011
Accepted 22 August 2011

Keywords:

Ceramics
Corrosion test
Energy dispersive analysis of X-rays
Microstructure

ABSTRACT

SmYbZr₂O₇ ceramic powders were pressureless-sintered at 1700 °C for 10 h to fabricate dense bulk materials. SmYbZr₂O₇ exhibited a single phase of defect fluorite-type structure. Hot corrosion tests between SmYbZr₂O₇ and V₂O₅ were carried out in an electric furnace at temperatures of 600–1000 °C for 2 h in air, respectively, and the reaction products were investigated using X-ray diffraction, laser Raman spectroscopy and scanning electron microscopy. The final corrosion products were composed of (Sm,Yb)VO₄ and ZrV₂O₇ or *m*-ZrO₂, depending upon the reaction temperature. Hot corrosion mechanisms were further discussed based on the thermal instability of ZrV₂O₇ at elevated temperatures.

© 2011 Elsevier B.V. All rights reserved.

1. Introduction

Ceramic thermal barrier coatings (TBCs) are usually used in gas turbines as thermal insulation to promote operating temperature and eventually enhance the engine efficiency [1,2]. Currently, the widely used TBC material is 6–8 wt.% Y₂O₃–ZrO₂ (YSZ). However, tetragonal zirconia is transformable to monoclinic phase upon cooling when the operating temperature is above 1200 °C, accompanied by a destructive volume change of 3–5%, which might lead to catastrophic failure of TBCs [3–6]. In recent years, rare-earth zirconates as potential TBCs materials have drawn great attention due to their attractive properties including low thermal conductivity (~1.4–2.0 W m⁻¹ K⁻¹, 20–1400 °C), high thermal expansion coefficient (~10.9 × 10⁻⁶ K⁻¹ at 1200 °C) and high thermochemical stability in high-temperature environment [7–12]. Therefore, rare-earth zirconate ceramics are excellent alternatives for applications of TBCs in engines.

When TBCs work in less-refined fuels with certain amounts of contaminant elements such as vanadium, sulfur, sodium or phosphorus, hot corrosion, as another key failure mode, becomes crucial and predominant to the environmental durability of TBCs materials [13–20]. During service, molten salts condense on the TBCs and react with the ceramic topcoat, leading to accelerated deterioration of TBCs. Among those impurities, chemical interactions between vanadium pentoxide and zirconia-based coatings are fastest and therefore the most deleterious [17,18]. As a result,

it is of great importance to explore a comprehensive understanding on vanadium-induced hot corrosion mechanism of rare-earth zirconates. Chen et al. studied the degradation of plasma-sprayed yttria-stabilized zirconia coatings via ingress of vanadium pentoxide at elevated temperatures. Phase evolution, from original corrosion product of ZrV₂O₇ to final decomposition product of *m*-ZrO₂, is found during the reaction between corrosive V₂O₅ and plasma-sprayed YSZ at 600–1000 °C [19]. Plasma sprayed La₂Zr₂O₇ coatings are relatively insusceptible to the attack by V₂O₅ at 1000 °C [20]. These coatings remain well bonded to the substrate after a high temperature exposure to V₂O₅, and exhibit a good stability in microstructures. However, hot corrosion mechanisms on reactions between SmYbZr₂O₇ and vanadium pentoxide were not well understood. The present work attempts to provide insight into hot corrosion behavior of SmYbZr₂O₇ ceramic with a thermal exposure to V₂O₅ salt at temperatures of 600–1000 °C for 2 h in air.

2. Experimental procedures

SmYbZr₂O₇ ceramic powders were prepared through chemical-coprecipitation and calcination method with zirconium oxychloride (Zibo Huantuo Chemical Co., Ltd., Huizhou, China; Analytical) and samarium oxide, ytterbium oxide powders (Rare-Chem Hi-Tech Co., Ltd., Beijing, China; purity ≥ 99.99%) as the starting materials. Details of the powder preparation process were given in our previous work [21]. The SmYbZr₂O₇ powders were molded by uniaxial stress, and the molded samples were further compacted by cold isostatic pressing method at 280 MPa for 5 min. The compacts were then pressureless-sintered at 1700 °C for 10 h at a heating rate of 5 °C min⁻¹ in air.

The specimens for hot corrosion tests were machined to the size of 10 mm × 10 mm × 3 mm from the as-sintered SmYbZr₂O₇ ceramic. The specimens were ground to 1500 grit finish, ultrasonically degreased in acetone, and dried at 100 °C over night. The V₂O₅ powder was uniformly spread over the surface of SmYbZr₂O₇ specimens to ensure a salt coverage of 20 mg cm⁻² using a very fine glass

* Corresponding author. Tel.: +86 451 86414291; fax: +86 451 86414291.
E-mail address: ouyangjh@hit.edu.cn (J.-H. Ouyang).

rod that was ultrasonically cleaned and dried. The V_2O_5 -coated $SmYbZr_2O_7$ specimens were placed in a zirconia crucible, which was subsequently covered with a thin zirconia sheet during heat-treatment. The V_2O_5 -coated $SmYbZr_2O_7$ specimens were isothermally heat-treated at temperatures of 600–1000 °C for 2 h in air. For a comparative Raman spectroscopic study on hot corroded products, hot corrosion tests of V_2O_5 -coated $Sm_2Zr_2O_7$ and $Yb_2Zr_2O_7$ samples were also performed at different temperatures of 600–1000 °C for 2 h to obtain $SmVO_4$ and $YbVO_4$, respectively.

Crystal structures of hot corroded specimens were identified by an X-ray diffractometer (Rigaku D/Max-2200VPC, Tokyo, Japan) operated at 30 kV and 25 mA with $Cu K\alpha$ radiation at a scan rate of 3° min^{-1} . The Raman spectra were collected with a microscopic confocal Raman spectrometer (Renishaw RM2000) using 632.8 nm (1.96 eV) laser excitation. The laser power of about 5 mW was used to collect the back-scattered Raman signal. The Raman signal was collected for 20 s for all specimens. The microstructural analysis of hot corroded specimens was carried out with a scanning electron microscope (FEI Quanta 200F, Eindhoven, the Netherlands) equipped with energy-dispersive X-ray spectroscopy operating at 30 kV. A thin gold film was evaporated onto the surface of hot corroded specimens for electrical conductivity prior to SEM observations.

3. Results and discussion

Fig. 1 shows XRD patterns obtained from the V_2O_5 -coated $SmYbZr_2O_7$ samples heat-treated at temperatures of 600–1000 °C in air. After hot corrosion tests at 600 °C for 2 h in air, the newly evolved peaks on the hot corroded surface include zirconium vanadate (ZrV_2O_7 , JCPDS no. 16-0422) and $(Sm,Yb)VO_4$, whose diffraction peaks are very close to the peaks of both samarium vanadate ($SmVO_4$, JCPDS no. 72-0279) and ytterbium vanadate ($YbVO_4$, JCPDS no. 72-0271). As the diffraction peaks of $SmVO_4$ and $YbVO_4$ phases overlap each other in the XRD pattern, an explicit determination for $(Sm,Yb)VO_4$ solid solution is quite difficult. However, the XRD results of hot-corroded samples obtained at temperatures of 700–1000 °C for 2 h are very similar, all of which demonstrate strong diffraction peaks of $(Sm,Yb)VO_4$ and weak peaks of monoclinic zirconia ($m\text{-}ZrO_2$, JCPDS no. 37-1484). Clearly, the diffraction peaks of $SmYbZr_2O_7$ are identified at all test temperature levels. As the thickness of the hot corrosion layer is smaller than the X-ray penetration depth, the diffraction peaks of the substrate $SmYbZr_2O_7$ are also detected. To further confirm the presence of $(Sm,Yb)VO_4$ solid solution instead of a possible mixture of $SmVO_4$ and $YbVO_4$ phases, laser Raman spectroscopy (LRS) studies were performed. For a comparative Raman spectroscopic study on hot corroded products, hot corrosion tests of V_2O_5 -coated $Sm_2Zr_2O_7$ and $Yb_2Zr_2O_7$ samples were also performed at different temperatures of 600–1000 °C for 2 h to obtain $SmVO_4$ and $YbVO_4$, respectively. Fig. 2 shows the Raman spectra of $SmVO_4$,

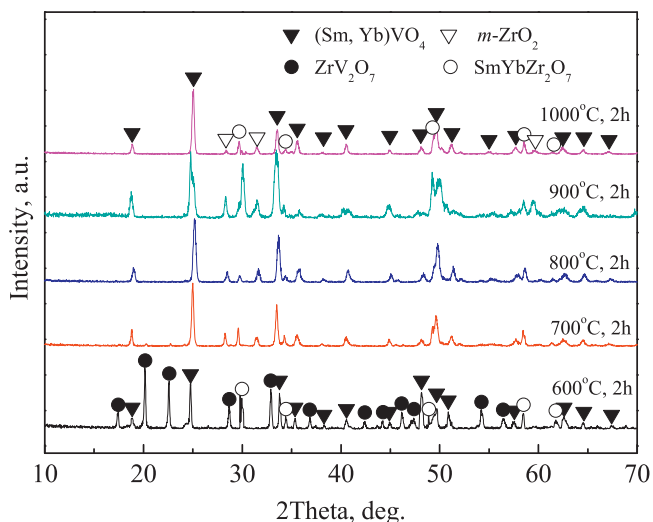


Fig. 1. XRD patterns of V_2O_5 -coated $SmYbZr_2O_7$ specimens heat-treated at temperatures of 600–1000 °C for 2 h in air.

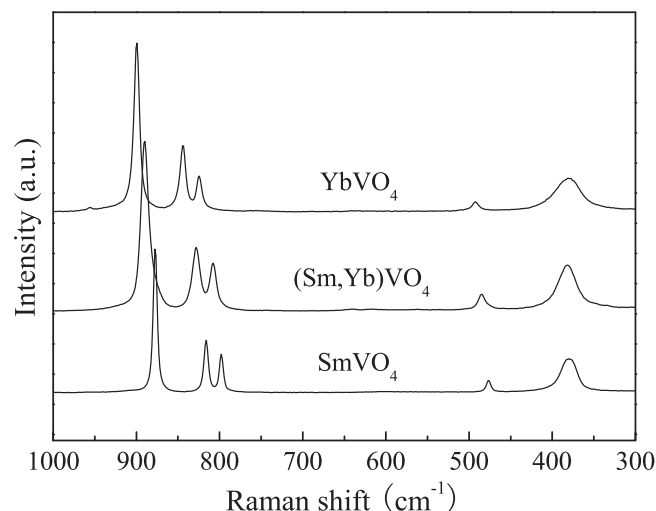


Fig. 2. Raman spectra of $SmVO_4$, $(Sm,Yb)VO_4$ and $YbVO_4$ hot corroded products.

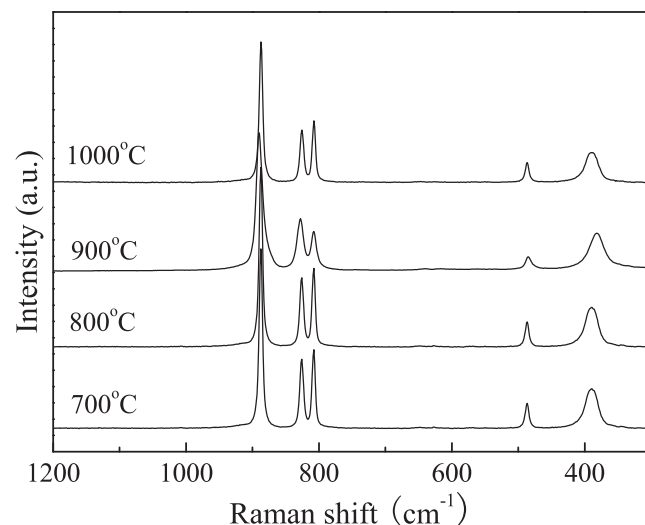


Fig. 3. Raman spectra of $(Sm,Yb)VO_4$ formed at temperatures of 700–1000 °C.

$(Sm,Yb)VO_4$ and $YbVO_4$ hot corroded products. As can be seen, Raman bands of $SmVO_4$ present at 878, 814, 811, 479 and 386 cm^{-1} , which are in good agreement with those reported in the literature [22]. The Raman spectrum of $YbVO_4$ shows all the characteristic bands [23]. From Fig. 2, Raman bands in $(Sm,Yb)VO_4$ spectrum lies between $SmVO_4$ and $YbVO_4$ spectra, instead of the overlapping of $SmVO_4$ and $YbVO_4$ spectra, which indicates that the solid solution of $SmVO_4$ and $YbVO_4$ is completely formed. Fig. 3 demonstrates Raman spectra of $(Sm,Yb)VO_4$ formed at temperatures of 700–1000 °C. No obvious Raman band shift is observed, which indicates that the phase composition keeps constant at different hot corrosion temperatures.

Fig. 4(a) shows typical surface morphology of the V_2O_5 -coated $SmYbZr_2O_7$ samples heat-treated at 600 °C for 2 h. Two kinds of different morphologies of hot corroded products are observed, marked as A and B in Fig. 4(a), respectively. Product A is block-shaped, while B is particle-shaped. EDS analysis in Fig. 4(b and c) identifies the compositions of different hot corroded products. In combination with the above XRD results, A is ZrV_2O_7 and B is $(Sm,Yb)VO_4$. As can be seen in region B, the particles are aggregative together, and their size is too small to be identified by EDS. SEM micrographs obtained on the surface of $SmYbZr_2O_7$ specimen after thermal exposure to the melt of V_2O_5 at 700 °C for 2 h, are

Download English Version:

<https://daneshyari.com/en/article/1523526>

Download Persian Version:

<https://daneshyari.com/article/1523526>

[Daneshyari.com](https://daneshyari.com)